Tractor driver psychological load evolution paradigm and experimental verification

Xiao Yang[1], Yaya Wang[1], Hongrui Hu[1], Weijie Guo[2*]
(1. *College of Engineering, China Agricultural University, Beijing 100083, China*;
2. *Ant Zhixin (Chengdu) Information Technology Co., Ltd., Chengdu 610041, China*)

Abstract: Developments in agricultural mechanization have witnessed a gradual transition from manned equipment to unmanned equipment. Meanwhile, the psychological load of the tractor drivers' original field operations has been transferred to unmanned tractor monitors. This study constructed a psychological load paradigm model and identified the physical meaning of parameters based on the leaky bucket principle and the basic hypothesis of ergonomics. The mapping architecture of the psychological load measurement principle was analyzed, and the feasibility of the questionnaire measurement method was demonstrated. Further, an evaluation questionnaire index system was designed. A continuous method was selected to conduct a man-machine semi-physical test to obtain an evolution paradigm model of six types of psychological loads using a multivariate nonlinear regression method. The structural parameters of the paradigm were analyzed, and the degree of coupling of psychological load generation and mitigation was deconstructed item by item. The driving mechanism and evolution law of psychological load were analyzed. Consequently, a real vehicle was designed and constructed and a topology test was conducted to verify the scientific applicability and universality of the paradigm model, respectively. The results confirmed that a continuous psychological questionnaire could effectively measure a driver's psychological load. The interaction of various psychological loads constituted the distributed state- space of psychological load, and the dynamic paradigm model drove the psychological load of the human-computer interaction interface. The paradigm model evolution was a negative exponential growth model that included comfort and fatigue accumulation rates. With the accumulation of working time, the specific rules and parameters of the psychological load changed for different drivers, but the evolution paradigm was the same. According to the state-space analysis of the mental load model, the mental model exhibited controllability, observability, stability, and so on, which accurately revealed the evolution law of mental load. The research results provide a positive design for human-computer interaction.

Keywords: psychological load mode, man-machine conflict, evolution paradigm, state-space, semi-physical experiment
DOI: 10.25165/j.ijabe.20251804.8885

Citation: Yang X, Wang Y Y, Hu H R, Guo W J. Tractor driver psychological load evolution paradigm and experimental verification. Int J Agric & Biol Eng, 2025; 18(4): 301–311.

1 Introduction

The psychological burden of "drivers" is an inherent aspect within agricultural technology transitioning towards unmanned systems, even though its form has evolved in various ways. Examples include human-operated tractors, remote-controlled tractors, unmanned tractors, tractor platform operators with "driver cabins", short-range operators, long-range operators, and remote monitors. These evolving roles face an inevitably common issue, which is human-machine conflicts during the human-machine interface interaction process. This necessitates the study of the evolutionary paradigm of psychological burden generation, alleviation, and accumulation in the human-machine interface interaction process for minimizing the psychological burden and designing interfaces that facilitate drivers to engage in efficient agricultural machinery operations for extended periods of time. This enables the monitors to respond promptly and accurately to unexpected program malfunctions in unmanned systems, coupled with efficient and accurate handling of emergencies.

In terms of psychological load test methods, Liu et al.[1] conducted real vehicle high-speed road tests based on the subtask method to study the characteristics of driver's psychological load. Wei et al.[2] conducted psychological load tests employing virtual roads and driving-simulation systems. Hu[3] conducted real-vehicle tests to study the changing characteristics of psychological loads in different highway tunnel sections. Young et al.[4] proposed and verified the effect of adaptive cruise control on the psychological load of drivers. Miao et al.[5] conducted a test of psychological load and danger perception in a simulated traffic environment. Karageorghis et al.[6] studied the interactive effects of task load and music rhythm on the psychological load through simulated driving experiments. In terms of psychological load model construction, Feng et al.[7] proposed a multibranch Long Short-Term Memory psychological load assessment model based on the attention mechanism. Zhang et al.[8] established a complex network model to predict the psychological load on air traffic control personnel. Kuriyagawa et al.[9] developed a mental workload assessment model. Fürstenau et al.[10] established a power-law model for the subjective psychological load, which was verified in a simulated environment.

Received date: 2024-09-27 **Accepted date:** 2025-03-16
Biographies: Xiao Yang, Associate Professor, research interest: ergonomics, Email: yangxiao2020@cau.edu.cn; **Yaya Wang**, MS, research interest: ergonomics, Email: 2697368288@qq.com; **Hongrui Hu**, undergraduate, research interest: Ergonomics, Email: 3119585935@qq.com.
***Corresponding author: Weijie Guo**, MS, research interest: ergonomics. Address: Room 1402, Building 15, No. 1999, Yizhou Avenue, High-tech Zone, Chengdu, Sichuan, China. Tel: +8618801002406, Email: guoweijie2406@163.com.

In the field of human-computer interaction interface design, Hao et al.[11] optimized the layout design of a driving cabin for domestic B-class SUVs. Li et al.[12] proposed a tractor cabin human-machine design evaluation model based on sensory ergonomics and an analytic hierarchy process. Chen et al.[13] improved the layout design of operating components such as steering wheels, instrument panels, and gear shift devices in automobiles. Francois et al.[14] revealed methods for improving automotive man-machine interface quality within the framework of cognitive ergonomics. Grandi et al.[15] designed ergonomic and usable instrument panels for tractors and trucks. Lu et al.[16] conducted a comprehensive design and evaluation of the human-machine interface of a certain type of loader using evaluation models. In terms of application of the state-space, Xie et al.[17] introduced a multi-degree-of-freedom structural system dynamic response analysis algorithm based on the state-space theory. Qiu et al.[18] established a unified digital model of wheelsets based on the state-space, realizing the digital identification and automated analysis of complex wheelsets. Yasrebi et al.[19] proposed a state-space-based optimization method to predict trajectory time characteristics using machine learning techniques. Based on the inverse theory of dynamic traffic volume, Zhao[20] constructs a state-space model for dynamic traffic volume prediction, and describes the Kalman filter algorithm.

This study aimed to address the problems of the unclear evolution paradigm of psychological load, unscientific psychological measurement methods, and impractical experimental verification in the human-computer interaction process[21]. The study constructed a psychological load paradigm model, proposed the mapping architecture of psychological load measurement and the measurement error analysis method, and analyzed the evolution rules of six types of psychological load using multivariate nonlinear regression and state-space methods based on semi-physical experimental data. Real-vehicle tests were conducted for validation. The research results attempted to solve the difficulties in the psychological measurement and quantification of psychological dynamics and provide a theoretical foundation for optimizing tractor control panels and remote monitoring platforms.

2 Paradigm model of psychological load evolution

2.1 Model assumptions

Psychological load refers to the load generated by the inherent load of the human-machine interface and the conflict between human cognitive processes. The psychological load can be alleviated in real time by an individual's psychological regulatory capacity. Thus, the psychological load borne by drivers is a composite load comprising inherent load, external interaction load, and the ability to alleviate the psychological load. According to a certain psychological paradigm and mechanism, the psychological load changes dynamically in real time and possesses the general characteristics of a system's dynamic state-space. Based on the principles of the leaky bucket algorithm[22], analyzing the process of psychological load generation, accumulation, and alleviation, a psychological load accumulation-alleviation model was proposed to analyze the psychological load evolution paradigm. The following assumptions are necessary for the model: 1) All types of psychological load are a form of "negative energy" that follows the law of energy conservation and can be operated mathematically. 2) All types of psychological load have an upper limit, namely, the psychological limit, and individuals can alleviate the psychological load on their own. This study considered an initial psychological load of 0. 3) According to the principle of superposition, the load exhibited by the operator is the "composite" load obtained by superimposing external, internal, and relevant loads.

2.2 Model establishment

Assuming that the driver is engaged in field mechanized operations, a certain part of the driver's body/a certain type of mental load/net mental load F generates load at a load rate $\omega(t)$. The corresponding comfort design delays the load generation with a "proportion rate" $c(t)$. As $c(t)$ reduces the existing load $F(t)$ by a certain proportional rate, it can be considered the load $c(t)\cdot F(t)\cdot \Delta t$ reduced from $F(t)$. Therefore, the load delaying rate should be $c(t)\cdot F(t)$. The load level of the driver at time t is denoted as $F(t)$, where, $F(0)=0$. A load analysis of the driver is shown in Figure 1.

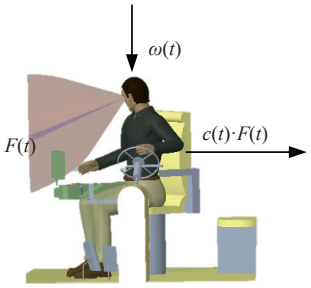

Figure 1 Driver human/psychological load analysis

Consider a small time increment $\Delta t>0$. During the time interval $[t, t+\Delta t]$, the driver's load accumulation is $\omega(t)\cdot\Delta t$. Comfort decreases the load by $c(t)\cdot F(t)\cdot\Delta t$. Therefore, the change in the driver's mental load within the time interval $[t, t+\Delta t]$ can be expressed as:

$$F(t+\Delta t)-F(t)=\omega(t)\times\Delta t-c(t)\times F(t)\Delta t \tag{1}$$

Considering the limit as Δt approaches zero on both sides of Equation (1), it could be obtained:

$$\frac{\mathrm{d}F(t)}{\mathrm{d}t}=\omega(t)-F(t)\times c(t) \tag{2}$$

According to the initial conditions of the model and the general solution formula for first-order nonhomogeneous linear differential equations, an integrated equation can be obtained as follows:

$$F(t)=\left[\int\omega(t)\exp\left(\int c(t)\mathrm{d}t\right)\mathrm{d}t-\int\omega(t)\exp\left(\int c(t)\mathrm{d}t\Big|_{t=0}\right)\right]\exp\left(-\int c(t)\mathrm{d}t\right) \tag{3}$$

To apply the model for problem analysis, this formula must be simplified. Assuming that the operating conditions are constant, the rate of increase in gross load and the rate of load relief are considered the average values, denoted as constants ω and c, respectively. This study aimed to investigate the regularity of the average load variation throughout the working stage of the driver. Equation (3), which serves as the expression for the psychological model in this study, can be simplified as follows:

$$F(t)=\frac{\omega}{c}(1-e^{-ct}) \tag{4}$$

2.3 Identification of the physical significance of the model

The model assumptions are validated as follows. In the mental workload model, $F(t)$ represents the net mental workload of the driver at a given moment, $c(t)$ denotes the comfort rate, and $\omega(t)$ represents the fatigue accumulation rate. Equation (4) indicates that when $t=0$, $F(t)=0$, which satisfies the initial conditions of the model construction. As time increases, $F(t)$ accumulates fatigue according to the growth pattern of the mental model. When t approaches infinity, $F(t)$ attains a constant upper bound.

The psychological-load characteristic parameters are identified as follows:

1) One of the coefficients of the mental model formula $-\frac{w}{c}e^{-ct}$. The net increase value of driver load is dimensionless, measured in s^{-1}, indicating that psychological load is accumulated by superimposing negative exponential norms.

2) One of the parameters of the mental model formula $\frac{w}{c}$. The upper limit value of the driver load is dimensionless and measured as 1, indicating the proportion of fatigue generation and fatigue relief degree to the total psychological capacity.

Based on the analysis of the identified physical meaning of psychological models, it can be concluded that the psychological load model constructed in this study conforms to the psychological laws of human beings and the characteristics of mental fatigue limits, and can represent the process of psychological fatigue accumulation and relief.

3 Human-machine semi-physical experimental measurement theory

3.1 Construction of psychological load index system

Based on cognitive load theory and the NASA-TLX subjective evaluation method, and referring to the architecture composition of Yang Si and Sheridan's psychological workload model[23], a psychological workload index evaluation system was established based on aspects such as emotional pressure, task pressure, and cognitive load[24,25], as shown in Figure 2.

The six primary factors were refined into a third-level index system serving as the 23-item questionnaire used in this research experiment.

3.2 Comparative analysis of sensory measurement methods

3.2.1 Mapping function of psychophysical measurement for mental workload

1) Psycho-physical-time function

In Figure 3, when operating human-machine systems, the complexity of external environmental dynamics and the inherent conflicts of the human-machine interface result in the generation of a temporal psychological fatigue load on the operator owing to external stimuli, constituting the psycho-physical-time function as follows:

$$f_i(t) = f[S_i(t)] \tag{5}$$

where, f_i is a psychological fatigue load generated in response to a physical stimulus acting on the operator. S_i is a physical stimulus intensity acting on the operator.

2) Questionnaire measuring psychological workload

The load of each question measured is: $X_i(t)$. The total psychological load is:

$$F(t) = F[f_1(t), f_2(t), \ldots, f_i(t)] = X[X_1(t), X_2(t), \ldots, X_i(t)] \tag{6}$$

3) Error propagation formula

This study only considered systematic errors and did not consider random errors and truncation errors. The error propagation equation is as follows:

$$\sigma_y^2 = \sum_{i=1}^{k} \left(\frac{\partial F}{\partial X_i}\right)^2 \sigma_{s_i}^2 \tag{7}$$

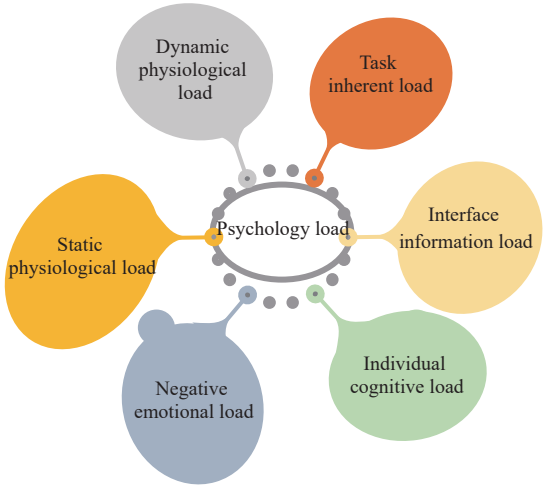

Figure 2 Psychological load index system

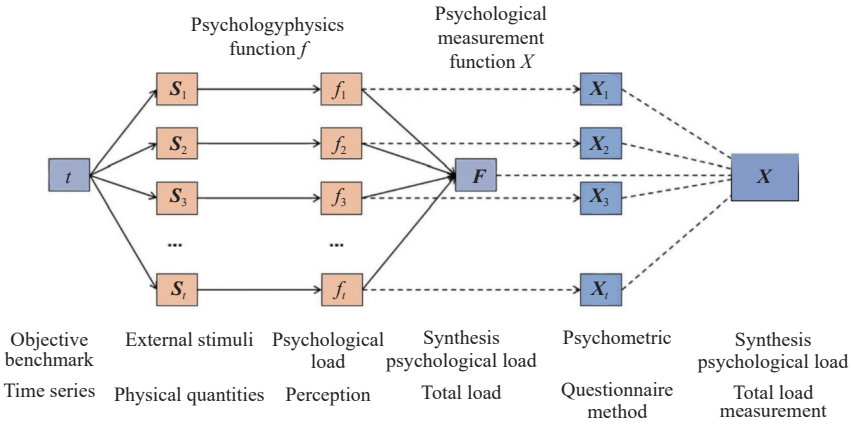

Figure 3 Mental load-physical measurement mapping

3.2.2 Measurement method configuration

A questionnaire with k questions is assumed, and each measures a subjective variable at t intervals. Each question has M sub-questions whose unit length is 1, and the total length of the line segment is M. The participant selects the red X point via the continuous method and the nearest N–1 point via the option method (Figure 4).

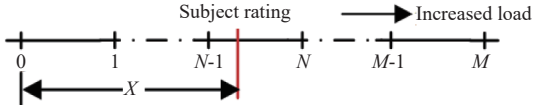

Figure 4 Questionnaire measurement options form

3.2.3 Comparison analysis between discrete method and continuous method

1) Definition and measurement method of the discrete method

and the continuous method

The discrete method refers to a method of calculating data wherein the values can only be natural numbers or integer units. The scores are calculated as follows:

$$S_{\mathrm{dn}} = N - 1 \tag{8}$$

The continuous method includes the score method and the proportion method. The score method uses the length of a marked line segment as the value. The score is represented as follows:

$$S_2 = X \tag{9}$$

The proportion method uses the ratio of the length of a marked line segment to the total length. The scores are calculated as follows:

$$S_3 = X/M \tag{10}$$

2) Error analysis of the discrete and continuous methods

Assuming that the participants are rational and cooperative during the experiment, significant errors are eliminated through electronic questionnaires. However, owing to the inherent flaws in the questionnaire design, systematic errors may still occur. Assuming that the true value of the psychological variable is x_{i0}, the error of the discrete method can be expressed as:

$$\sigma_{S_i} = S_i - x_{i0} \tag{11}$$

As for the continuous method, when calculating the score and proportion values, the computer may generate infinite nonrecurring decimals or recurring decimals. In this case, the decimal points must be rounded off to two decimal places, which results in truncation errors.

Only systematic errors in psychological measurements are considered, excluding random and truncated errors. By substituting the relevant variables into the error propagation formula as expressed in Equation (7), the error formula for the scoring method and the error formula can be respectively obtained as Equations (12) and (13):

$$\sigma_{S_{2y}}^2 = \sum_{i=1}^{k} \left(\frac{\partial F}{\partial X_i}\right)^2 (X_i - x_{i0})^2 \tag{12}$$

$$\sigma_{S_{3y}}^2 = \sum_{i=1}^{k} \left(\frac{\partial F\left(\frac{X_i}{M}\right)}{\partial \frac{X_i}{M}} \frac{\mathrm{d}\left(\frac{X_i}{M}\right)}{\mathrm{d}X_i}\right)^2 \left(\frac{X_i - x_{i0}}{M}\right)^2 = \frac{\sigma_{S_{2y}}^2}{M^4} \tag{13}$$

Based on the two equations above, it can be concluded that for the overall mental workload function, the proportional method exhibits the smallest error, which is M^4 times smaller than that of the discrete method. Furthermore, as the number of options for each question increases, the error gradually decreases. Currently, in the field of mental workload measurement, the number of measurement options has gradually increased from three or five options to nine or 11 options, respectively, indicating that the traditional discrete option method is transitioning and exploring a continuous method. This study further validated this developmental pattern and demonstrated the validity of the continuous measurement methods.

Moreover, psychological workload is a continuous numerical variable. Therefore, a continuous method is required for psychological measurements. The degree of psychological workload is converted into scores ranging from 0-1. To a certain extent, the score method reflects the numerical value of the psychological workload. Both methods used the same measurement scale and can be represented using appropriate measurement methods.

3.3 Human-machine hybrid experiment design

3D modeling, simulation, and model production were carried out. A suitable experimental prototype was selected, and the operation platform was assembled to complete the construction of the experimental test bench, as shown in Figure 5.

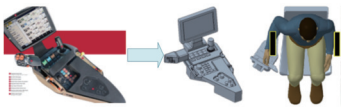

a. 3D modeling and posture simulation of typical poducts

b. External of human-machine semi physical test bench

c. Simulate homework scenarios

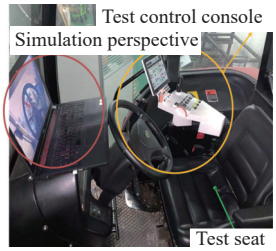

d. Inside the human-machine semi physical test bench

Figure 5 Man-machine semi-physical test bench

Based on the basic principles and considerations of the psychological load experiments, a detailed experimental procedure was formulated, as shown in Figure 6.

The male-to-female ratio of tractor drivers in China generally ranges from 9:1 to 19:1[26]. Therefore, in this indoor experiment, 11 adult males with driving experience and one adult female were selected as subjects. The experiment included data collection of timed psychological workload questionnaires at four time points: 5, 10, 15, and 20 min. A total of 12 sessions and 48 valid questionnaires were collected in this experiment.

4 Analysis of the evolutionary patterns of psychological stress

4.1 Psychological load-time function fitting

Cronbach's alpha coefficient[27] of the questionnaire was calculated ranging from 0.7-0.8. This demonstrated the scientific and feasible nature of the experimental questionnaire.

The average data for each item at the four time points were calculated for all 12 participants. Based on the psychological load model using Equation (4), MATLAB software was used to fit and simulate the psychological load curves under temporal changes. A total of 23 fitting equations and indices were obtained, as listed in Table 1. The 23 fitting curves are displayed in Figure 7.

The coefficient of determination R^2 reflects the percentage of variance in the dependent variable, which can be explained by a regression equation. As shown in Table 1, the fitting equations can explain 80%–93% of the variance in the dependent variable, indicating good performance. By examining the 23 fitting curves in Figure 7, it can be observed that the fitting effect of the experimental data is consistent with the trend pattern of the psychological model in this study.

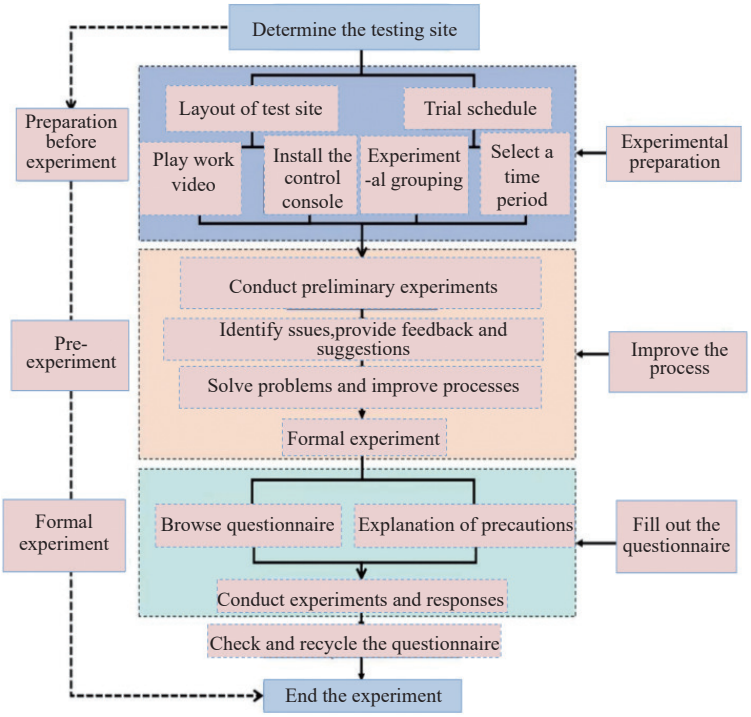

Figure 6 Test flow chart

Table 1 Fitting equation and fitting index table

Number	Fitting equation	R^2
1	$F(t)=0.812(1-e^{-0.051t})$	0.8552
2	$F(t)=0.78(1-e^{-0.073t})$	0.8400
3	$F(t)=1.80(1-e^{-0.017t})$	0.9246
4	$F(t)=1.076(1-e^{-0.033t})$	0.8703
5	$F(t)=1.21(1-e^{-0.030t})$	0.8677
6	$F(t)=2.14(1-e^{-0.013t})$	0.8737
7	$F(t)=0.73(1-e^{-0.057t})$	0.8758
8	$F(t)=1.03(1-e^{-0.035t})$	0.9054
9	$F(t)=0.77(1-e^{-0.050t})$	0.8371
10	$F(t)=0.78(1-e^{-0.055t})$	0.9157
11	$F(t)=0.64(1-e^{-0.099t})$	0.8647
12	$F(t)=0.95(1-e^{-0.042t})$	0.8692
13	$F(t)=0.78(1-e^{-0.058t})$	0.8953
14	$F(t)=0.77(1-e^{-0.060t})$	0.7837
15	$F(t)=0.86(1-e^{-0.068t})$	0.8633
16	$F(t)=0.76(1-e^{-0.061t})$	0.7820
17	$F(t)=1.37(1-e^{-0.027t})$	0.8357
18	$F(t)=2.29(1-e^{-0.016t})$	0.7919
19	$F(t)=0.71(1-e^{-0.066t})$	0.8012
20	$F(t)=1.09(1-e^{-0.043t})$	0.8539
21	$F(t)=0.73(1-e^{-0.063t})$	0.8202
22	$F(t)=0.88(1-e^{-0.053t})$	0.8164
23	$F(t)=1.00(1-e^{-0.048t})$	0.8523

4.2 Analysis of the evolutionary characteristics of psychological load

Relevant statistical measures for the rates of increase and relief of psychological load are presented in Table 2.

As shown in Table 2, the average values of the ω load increase rate ranged from 0.0320-0.0557, and the average values of the c load relief rate ranged from 0.0210-0.0675 for each secondary indicator. Considering that the ω load increase rate must be within a psychologically controllable range, it can reduce the production of psychological fatigue when it is below the 25th percentile. The value of the load-relief rate c should be relatively large. In the design, c should exceed the 75th percentile, which can significantly accelerate

Table 2 Load increase and mitigation rate statistics

Category	Statistic	c	ω
Intrinsic load of task content (Questions 1-4)	Mean	0.0435	0.0413
	25th percentile	0.0210	0.0323
	50th percentile	0.0420	0.0385
	75th percentile	0.0675	0.0530
Interface information load (Questions 5-9)	Mean	0.0370	0.0362
	25th percentile	0.0215	0.0320
	50th percentile	0.0350	0.0360
	75th percentile	0.0535	0.0405
Individual cognitive load (Questions 10-12)	Mean	0.0653	0.0487
	25th percentile	0.0420	0.0400
	50th percentile	0.0550	0.0430
	75th percentile	0.0770	0.0530
Negative emotional load (Questions 13-16)	Mean	0.0618	0.0490
	25th percentile	0.0585	0.0453
	50th percentile	0.0605	0.0460
	75th percentile	0.0663	0.0557
Static physiological load (Questions 17-20)	Mean	0.0380	0.0420
	25th percentile	0.0188	0.0370
	50th percentile	0.0350	0.0420
	75th percentile	0.0603	0.0470
Dynamic physiological load (Questions 21-23)	Mean	0.0547	0.0470
	25th percentile	0.0480	0.0460
	50th percentile	0.0530	0.0470
	75th percentile	0.058	0.0475
Total load	Mean	0.0470	0.0418
	25th percentile	0.0300	0.0300
	50th percentile	0.0510	0.0510
	75th percentile	0.0610	0.0610

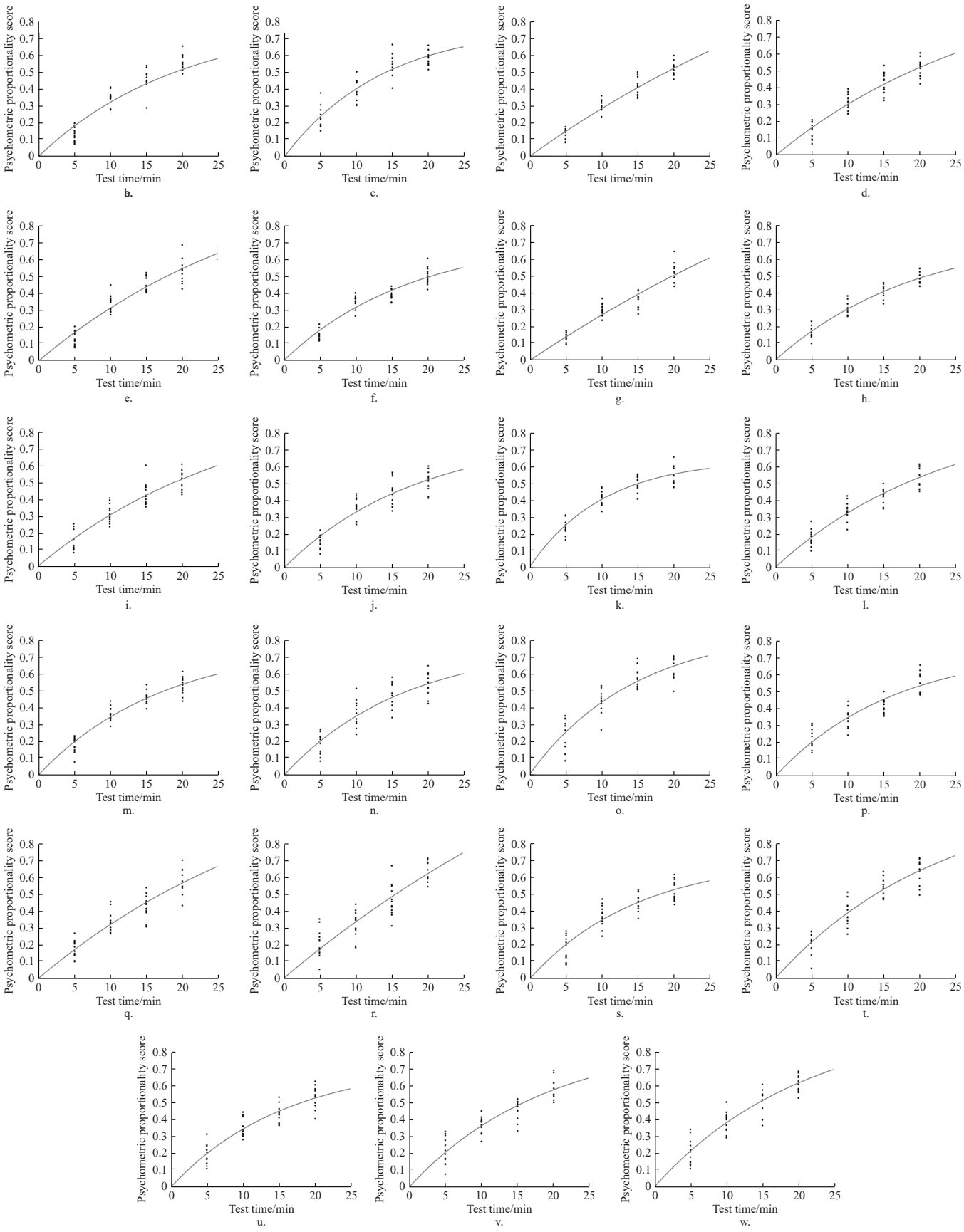

Figure 7 Psychological load curve fitting diagram

the load relief and reduce the accumulation of psychological load. Based on the distribution characteristics of load increase and relief rates shown in Table 2, a comparison of load increase and relief levels is illustrated in Figure 8.

From the radar chart of the load increase and load relief rates, it can be observed that the load increase and relief rates of the intrinsic load and interface information load are the most similar, indicating that the increase in load is accompanied by a relatively small accumulation of load, similar to the approximate load amount. However, the relief rate of individual cognitive and negative

emotional loads is greater than the load generation rate, indicating that these two types of loads can be quickly relieved through individual psychological regulation without a long-term impact on the driver's physical and mental state. The load increase rate of the static physiological load exceeded the relief rate, indicating that it was long-lasting in relation to the static physiological load, and could only significantly attenuate and disappear after the work ceased. Fatigue can accumulate during work, resulting in lower relief rates. The relief rate of the dynamic physiological load was slightly greater than the load increase rate, because, compared to the static physiological load, dynamic situations involved fluctuations, vibrations, and changes and were greatly influenced by the environment. Therefore, the relief rate of this load was higher than that of a static physiological load, thereby providing an opportunity for release and relief under contextual influences.

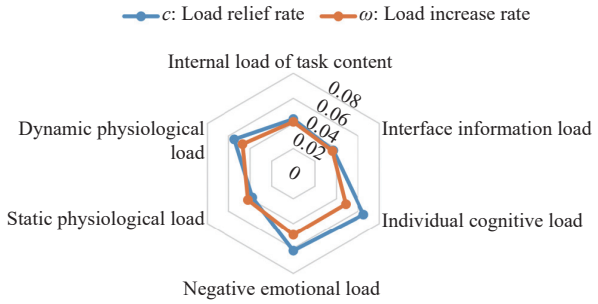

Figure 8 Load increase and mitigation rate radar chart

A comparison of the results of various secondary indicators of psychological workload revealed that the mean relief rate of individual cognitive workload was the highest (0.0653) and that of interface information workload was the lowest (0.0370). This is because the individual cognitive workload is the psychological fatigue generated by complex decision-making and frequent operations during agricultural machinery operations; however, it can be effectively alleviated through the gradual completion of the current agricultural machinery operation task, gradual proficiency in operating procedures, and a pleasant agricultural natural environment. This can induce a self-situational regulation effect, thus effectively relieving cognitive workload. However, the interface information workload is generated by the inherent design level of the human-machine interface, and it cannot be effectively alleviated through self-regulation by the driver. Therefore, the relief rate is the lowest. In terms of the rate of psychological workload generation, the mean rate of negative emotional workload generation was the highest (0.0490), whereas the mean rate of interface information workload generation was the lowest (0.0362). This is because all psychological workloads undertaken by drivers during agricultural machinery operation can trigger the accumulation and superposition of negative emotions, resulting in a higher rate of negative emotional workload generation. However, the human-machine interface design was fixed and its workload accumulation was not affected by the cross-interference of other psychological workloads, resulting in the lowest and most stable rate of workload generation.

4.3 Analysis of psychological load state-space

The average load increase and the average load relief rates, denoted as $\omega(t)$ and $c(t)$ respectively, are undetermined parameters obtained by fitting the experimental data to the psychological load model curve. In the state-space analysis, both parameters are assumed to be constant, indicating that the system is a linear time-invariant system.

4.3.1 Controllability analysis of the system

Controllability reflects the influence of input signals on the system state and its control capability[28].

Analysis of controllability:

$$B=\begin{pmatrix}1\\1\\1\\1\end{pmatrix};\ A=\begin{pmatrix}-0.051 & 0 & 0 & 0\\ 0 & -0.073 & 0 & 0\\ 0 & 0 & \cdots & 0\\ 0 & 0 & 0 & -0.048\end{pmatrix};$$

$$AB=\begin{pmatrix}-0.051\\-0.073\\\vdots\\-0.048\end{pmatrix}$$

$$A^2=\begin{pmatrix}0.0026 & 0 & 0 & 0\\ 0 & 0.0053 & 0 & 0\\ 0 & 0 & \cdots & 0\\ 0 & 0 & 0 & 0.0023\end{pmatrix};$$

$$A^2B=\begin{pmatrix}0.0026\\0.0053\\\vdots\\0.0023\end{pmatrix}$$

$$\mathrm{rank}Q=\mathrm{rank}\left(B\ \ AB\ \ A^2B\ \ \cdots\ \ A^{n-1}B\right)=\begin{pmatrix}1 & -0.051 & \cdots & 0.051^{22}\\ 1 & -0.073 & \cdots & 0.073^{22}\\ \vdots & \vdots & \cdots & \vdots\\ 1 & -0.048 & \cdots & 0.048^{22}\end{pmatrix} \tag{14}$$

$$\mathrm{rank}Q=23=n \tag{15}$$

The state of the system is fully controllable, and the internal state variables x of the system can be influenced by the inputs, starting from any initial state at any given initial time, and can be controlled to the system origin within a finite time.

1) Analysis of output controllability

$$\mathrm{rank}=\mathrm{rank}\left(CB\ \ CAB\ \ \cdots\ \ CA^{n-1}B\ \ D\right)=1=m \tag{16}$$

The rank of the controllability matrix equals the dimensions of the output variables, so the system is completely controllable.

4.3.2 Systematic observability analysis

State observability reflects the ability to determine or identify the system state from directly or indirectly measurable outputs $y(t)$ and inputs $u(t)$ from an external system[28].

$$Q_0=\begin{pmatrix}C\\CA\\\vdots\\CA^{n-1}\end{pmatrix}=\begin{pmatrix}C\\CA\\\vdots\\CA^{22}\end{pmatrix} \tag{17}$$

$$Q_0=\begin{pmatrix}1 & 1 & \cdots & 1\\ -0.051 & -0.073 & \cdots & -.048\\ \vdots & \vdots & \cdots & \vdots\\ (-0.051)^{22} & (-0.073)^{22} & \cdots & (-0.048)^{22}\end{pmatrix} \tag{18}$$

$$\mathrm{rank}Q_0=23=n \tag{19}$$

The proportion method yields fractions, and the last several

rows of Q_0 tend towards zero. However, the measurement results using proportion can be simultaneously enlarged by a certain multiple for calculation. Therefore, the rank of Q_0 is 23, which is equal to the dimension of the system state variable n. Consequently, the system state can be fully observed. In other words, changes in the psychological load state can be uniquely determined by the external inputs and outputs of the system.

4.3.3 System stability analysis

Lyapunov stability refers to the ability of a system to return to its equilibrium state after a disturbance for a "sufficiently long" period of time[29]. The stability analysis of a system can be conducted using Lyapunov algebraic equations, which are represented as follows:

$$PA + A^{\mathrm{T}}P = -I \tag{20}$$

$$A = \begin{pmatrix} -c_1 & 0 & 0 & 0 \\ 0 & -c_2 & 0 & 0 \\ 0 & 0 & \cdots & 0 \\ 0 & 0 & 0 & -c_{23} \end{pmatrix} \tag{21}$$

$$P = \begin{pmatrix} P_{11} & P_{12} & \cdots & P_{1n} \\ P_{12} & P_{22} & \cdots & P_{2n} \\ \vdots & \vdots & \cdots & \vdots \\ P_{1n} & P_{2n} & \cdots & P_{nn} \end{pmatrix} \tag{22}$$

Substituting P into the Lyapunov equation yields:

$$P\begin{pmatrix} -c_1 & 0 & 0 & 0 \\ 0 & -c_2 & 0 & 0 \\ 0 & 0 & \cdots & 0 \\ 0 & 0 & 0 & -c_{23} \end{pmatrix} + \begin{pmatrix} -c_1 & 0 & 0 & 0 \\ 0 & -c_2 & 0 & 0 \\ 0 & 0 & \cdots & 0 \\ 0 & 0 & 0 & -c_{23} \end{pmatrix} P = -\begin{pmatrix} 1 & 0 & 0 & 0 \\ 0 & 1 & 0 & 0 \\ 0 & 0 & \cdots & 0 \\ 0 & 0 & 0 & 1 \end{pmatrix} \tag{23}$$

$$\begin{pmatrix} -c_1P_{11} & -c_2P_{12} & \cdots & -c_{23}P_{1n} \\ -c_1P_{12} & -c_2P_{22} & \cdots & -c_{23}P_{2n} \\ \vdots & \vdots & \cdots & \vdots \\ -c_1P_{1n} & -c_2P_{2n} & \cdots & -c_{23}P_{nn} \end{pmatrix} + \begin{pmatrix} -c_1P_{11} & -c_1P_{12} & \cdots & -c_1P_{1n} \\ -c_2P_{12} & -c_2P_{22} & \cdots & -c_2P_{2n} \\ \vdots & \vdots & \cdots & \vdots \\ -c_{23}P_{1n} & -c_{23}P_{2n} & \cdots & -c_{23}P_{nn} \end{pmatrix} = -\begin{pmatrix} 1 & 0 & 0 & 0 \\ 0 & 1 & 0 & 0 \\ 0 & 0 & \cdots & 0 \\ 0 & 0 & 0 & 1 \end{pmatrix} \tag{24}$$

$$\begin{pmatrix} -2c_1P_{11} & -c_2P_{12}-c_1P_{12} & \cdots & -c_{23}P_{1n}-c_1P_{1n} \\ -c_1P_{12}-c_2P_{12} & -2c_2P_{22} & \cdots & -c_{23}P_{2n}-c_2P_{2n} \\ \vdots & \vdots & \cdots & \vdots \\ -c_1P_{1n}-c_{23}P_{1n} & -c_2P_{2n}-c_{23}P_{2n} & \cdots & -2c_{23}P_{nn} \end{pmatrix} = -\begin{pmatrix} 1 & 0 & 0 & 0 \\ 0 & 1 & 0 & 0 \\ 0 & 0 & \cdots & 0 \\ 0 & 0 & 0 & 1 \end{pmatrix} \tag{25}$$

$$P = \begin{pmatrix} 1/2c_1 & 0 & \cdots & 0 \\ 0 & 1/2c_2 & \cdots & 0 \\ \vdots & \vdots & \cdots & \vdots \\ 0 & 0 & \cdots & 1/2c_{23} \end{pmatrix} = \frac{1}{2}\begin{pmatrix} c_1 & 0 & \cdots & 0 \\ 0 & c_2 & \cdots & 0 \\ \vdots & \vdots & \cdots & \vdots \\ 0 & 0 & \cdots & c_{23} \end{pmatrix} \tag{26}$$

It is obtained that P is a diagonal matrix (a matrix in which all elements except the diagonal elements are zero). It must be positive definite. Therefore, the system is asymptotically stable in the large. At this time, the Lyapunov function of the system and its total derivative with respect to time t along the state trajectory are respectively:

$$V(x) = x^{\mathrm{T}}Px = \frac{1}{2}x^{\mathrm{T}}\begin{pmatrix} c_1 & 0 & \cdots & 0 \\ 0 & c_2 & \cdots & 0 \\ \vdots & \vdots & \cdots & \vdots \\ 0 & 0 & \cdots & c_{23} \end{pmatrix} x > 0 \tag{27}$$

$$\dot{V}(x) = -x^{\mathrm{T}}Qx = x^{\mathrm{T}}\begin{pmatrix} -1 & 0 & 0 & 0 \\ 0 & -1 & 0 & 0 \\ 0 & 0 & \cdots & 0 \\ 0 & 0 & 0 & -1 \end{pmatrix} x < 0 \tag{28}$$

The aforementioned function calculation demonstrates that in this system, the driver's psychological state can undergo self-recovery and fatigue relief over time after being subjected to certain disturbances, ultimately returning to a normal physical and mental state.

4.4 Analysis of the paradigm of psychological load evolution

In summary, the deconstruction of the psychological load evolution paradigm for drivers during plowing operations was as follows:

1) The generation of psychological load. First, complex agricultural working conditions combined with external operational environmental interference cause drivers to experience attention allocation conflicts, resulting in a division of attention between the control panel and the external environment. Owing to inherent cognitive differences between the interface and the driver's cognitive patterns, human-machine conflicts arise during interface interactions.

2) Mechanism driving psychological load. An external load is the type of load that humans experience when subjected to external stimuli, which results in a psychological load owing to attention allocation conflicts caused by agricultural work environments. Internal load is related to the design level of the human-machine interface, that is, the inherent cognitive patterns of the control panel conflict with those of the driver, resulting in a psychological load. These two types of loads are distributed in several ways and interact with each other, forming a distributed state-space of the psychological load and driving the psychological load dynamics paradigm model of the human-machine interaction interface.

3) The evolution paradigm of psychological load. During the working process, the psychological load continuously increases objectively, and psychological regulation occurs autonomously, resulting in a "leaky bucket" effect. By constructing a "leaky bucket" model, the paradigm model of psychological load generation and relief rates can be obtained, which includes the proportion of psychological load generation and relief levels to the total psychological capacity $\frac{w}{c}$ and the net increase value $-\frac{w}{c}e^{-ct}$. The analysis framework of the psychological load evolution paradigm is shown in Figure 9 below.

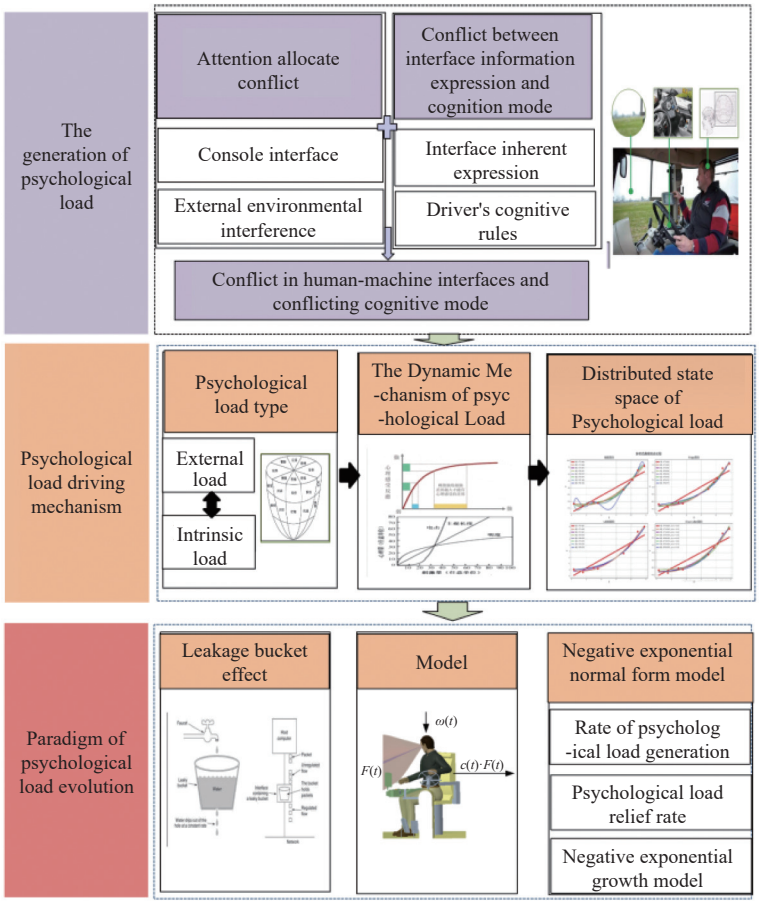

Figure 9 Analysis of psychological load evolution paradigm

5 Experimental validation of the actual vehicle

5.1 Experimental procedure

A farm in the Pinggu District, Beijing, was selected as the test site. A large Dongfanghong tractor, which was the same brand as the indoor test prototype, was selected as the test vehicle. Two experienced agricultural machinery operators were selected to perform actual plowing operations and stopped driving at four time points (5, 10, 15, and 20 min) for questionnaire measurements. The test control console used in the indoor test was installed in the test tractor. Photographs of the actual vehicle tests are shown in Figure 10.

Figure 10 Real vehicle test pictures

5.2 Experimental verification of theoretical paradigms

The experimental data were organized and four random items were input to the psychological model. A psychological-load curve-fitting simulation was conducted, and the fitted equation and index table are listed in Table 3. The determination coefficients (R-squared values) for curves (a)-(d) all exceeded 0.8, indicating that they could represent and explain more than 80% of the variation in the dependent variable. The fitted curve shown in Figure 11 indicated that the psychometric data still conformed to the temporal variation pattern of the psychological load model.

Table 3 Real vehicle test fitting equation and index table

Number	Fitting equation	R^2
3	$F(t)=0.65(1-e^{-0.090t})$	0.8350
9	$F(t)=0.74(1-e^{-0.073t})$	0.8381
12	$F(t)=1.72(1-e^{-0.023t})$	0.8514
23	$F(t)=0.83(1-e^{-0.069t})$	0.8153

The results of the actual vehicle tests indicated that the curve-fitting index was relatively high. The psychophysiological load evolution paradigm constructed in this study can characterize the change patterns of human operators' psychological loads in actual operational scenarios at the same control station, demonstrating its reliability and scientific validity.

5.3 Topological experimentation and paradigm validation

A control panel with a changed appearance, structure, and color was used to conduct a topology experiment. The original experimental control panel and the topology one are shown in Figure 12e on the left in black and on the right in white, respectively.

The fitted equation and fitting index of the topology test are

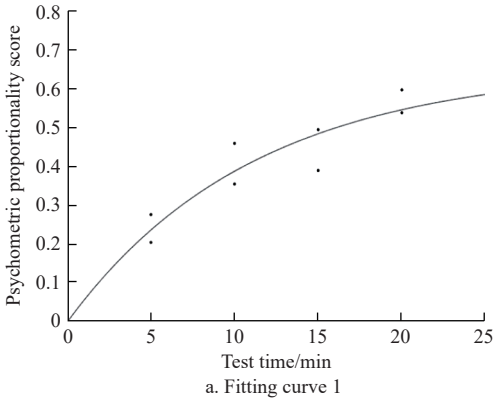

a. Fitting curve 1

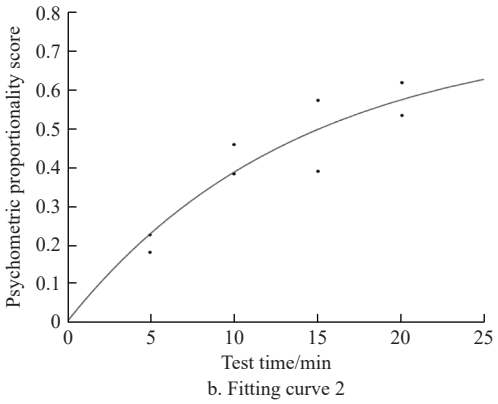

b. Fitting curve 2

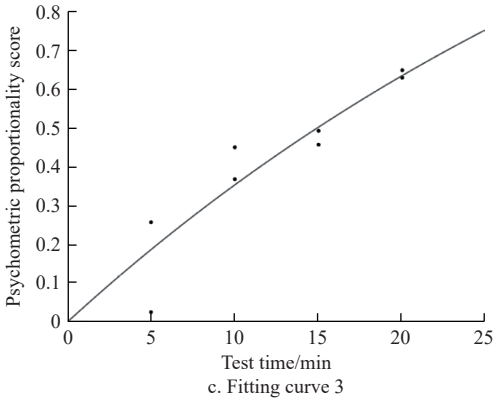

c. Fitting curve 3

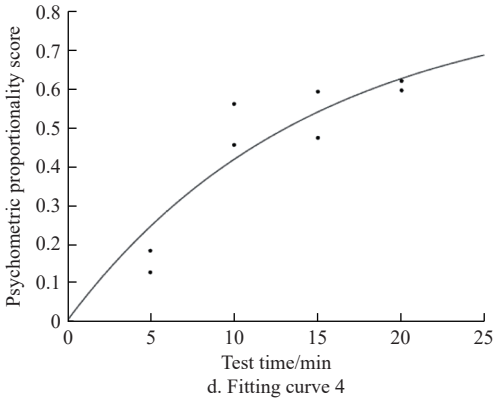

d. Fitting curve 4

Figure 11 Real vehicle test fitting curve

listed in Table 4, where the curves in Figures 12a-12d all had a determination coefficient greater than 0.75. This indicated that the topology test can characterize and explain more than 75% of the variation in the dependent variable.

The fitted curves are shown in Figures 12a–12d. The psychometric data obtained in the topological experiment still conformed to the temporal variation pattern of the psychological load model established in this study.

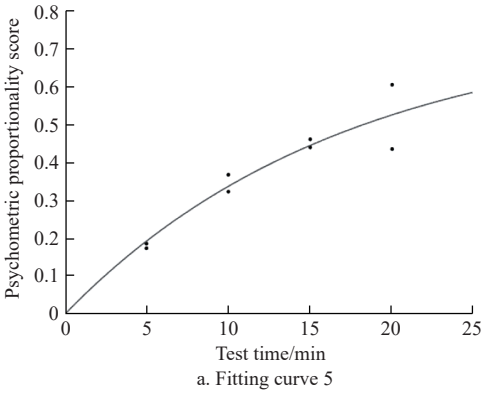

a. Fitting curve 5

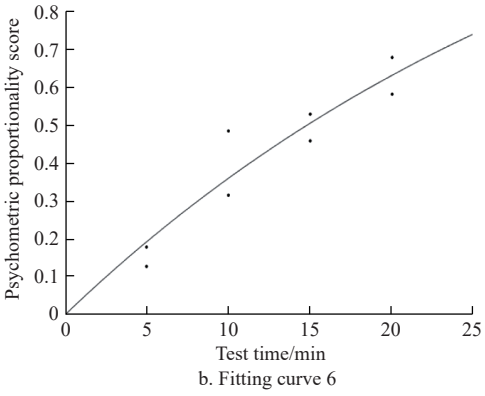

b. Fitting curve 6

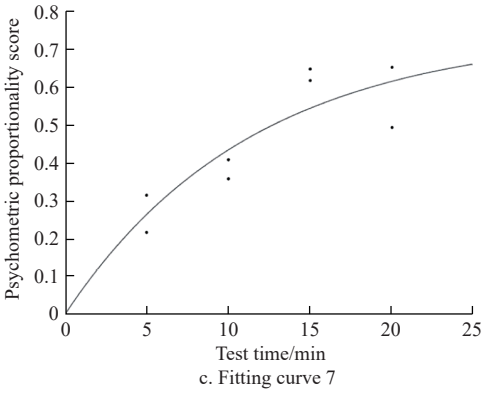

c. Fitting curve 7

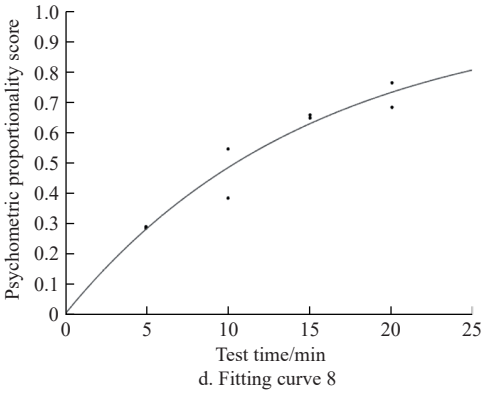

d. Fitting curve 8


e. Original experimental conscle and topology experimental consale

Figure 12 Topology test fitting curve and control console comparison diagram

Table 4 Topology test fitting equation and index table

Number	Fitting equation	R^2
5	$F(t)=0.76(1-e^{-0.058t})$	0.8895
7	$F(t)=0.67(1-e^{-0.090t})$	0.8290
14	$F(t)=1.45(1-e^{-0.053t})$	0.8894
20	$F(t)=0.74(1-e^{-0.088t})$	0.7725

The results of the topological experiment indicate that the psychological model established in this study can characterize the variation pattern of the mental workload of operators in different types of control stations in real operational scenarios.

6 Conclusions

1) Continuous psychological questionnaires were found to effectively measure the psychological workload of drivers. Compared with traditional discrete option questionnaires, the relative error multiplier of the continuous questionnaires was reduced by a factor of M^4.

2) The psychological workload evolution paradigm followed a negative exponential growth model. In the model, $c(t)$ represents the comfort rate and $\omega(t)$ represents the fatigue accumulation rate. With the accumulation of working time, different drivers exhibited different patterns of psychological workload changes, and the undetermined parameters of the psychological model were also different; however, the evolution patterns were the same.

3) Based on the state-space analysis of the psychological workload model, it was observed that the psychological model possessed controllability, observability, stability, and other state-space characteristics, which align with the fundamental characteristics of psychological workload changes and can accurately reveal the evolution patterns of psychological workload.

Acknowledgements

This research was supported by the National Natural Science Foundation of China (Grant No. 32201671).

[References]

[1] Liu Z F, Ding T, Wu F W, Zhang H L. Impact of level-2 autonomous driving mode on drivers' mental workload under low traffic volume of straight motorway. Journal of China Highway, 2022; 35(4): 256–266.

[2] Wei W H. Influence of lane reduction on driving behavior characteristics under multi-factor interaction. Journal of Chang'an University (Natural Science Edition), 2020; 40(4): 117–126.

[3] Hu Y Q. Study on drivers' mind wandering, mental workload and safety risks in highway tunnels. PhD dissertation. Xi 'an: Chang'an University, 2021; 6. 183p. doi: 10.26976/d.cnki.gchau.2021.000040 (in Chinese)

[4] Young M S, Stanton N A. Taking the load off: investigations of how adaptive cruise control affects mental workload. Ergonomics: The official publication of the Ergonomics Research Society, 2004; 47(9): 1014–1035.

[5] Miao L Q, Gu Y J, He L C, Wang H R, Schwebel D C, Shen Y J. The influence of music tempo on mental load and hazard perception of novice drivers. Accident Analysis and Prevention, 2021; 157(7): 106168.1–106168.6.

[6] Karageorghis C I, Kuan G, Mouchlianitis E, Payre W, Howard L W, Reed N, et al. Interactive effects of task load and music tempo on psychological, psychophysiological, and behavioural outcomes during simulated driving. Ergonomics: The official publication of the Ergonomics Research Society, 2022; 65(7): 915–932.

[7] Feng Y, Li Y L, Li Y F, Zhang B, Ding J H, Xia L K. Novel multiclass classification framework with muti-branch LSTM and attention mechanism for mental workload evaluation. Computer Application Research, 2021; 38(11): 3371–3375.

[8] Zhang J Y, Qiao H, E X T. A new way to predict the psychological load of air traffic controllers: the associated complexity network model. Beijing; Institute of Psychology, Chinese Academy of Sciences, 2020-12-31.

[9] Kuriyagawa Y, Kageyama I. A study on evaluation method for driver-vehicle-environment system using the mental work load. In: World Automotive Congress (FISITA 2002). Helsinki. 2002; pp.525–532.

[10] Fürstenau N, Radüntz T. Power law model for subjective mental workload and validation through air traffic control human-in-the-loop simulation. Cognition, Technology & Work, 2022; 24(2): 291–315.

[11] Hao S, Cheng C T, Wang J N, Zhang J Y, Yu Y. Ergonomic optimization and test evaluation of sports SUV cockpit layout design. Journal of Jilin University (Engineering Edition), 2022; 52(7): 1477–1488.

[12] Li Y H, Yang X, Zhu H, Yang G H. Evaluation study on man-machine design of tractor cab based on KE and AHP theory. Shandong Agricultural Mechanization, 2022; 351(4): 35–36, 41.

[13] Chen D K, Guo J Y, Wang J L, Li Z, Li F Z. Research on ergonomics improvement design of automobile cab based on CATIA. Mechanical Design, 2019; 36(9): 127–131.

[14] Francois M, Osiurak F, Fort A, Crave P, Navarro J. Automotive HMI design and participatory user involvement: review and perspectives. Ergonomics: The official publication of the Ergonomics Research Society, 2017; 60(4): 541–552.

[15] Grandi F, Prati E, Peruzzini M, Pellicciari M, Campanella C E. Design of ergonomic dashboards for tractors and trucks: innovative method and tools. Journal of Industrial Information Integration, 2022; 25. doi: 10.1016/J.JII.2021.100304

[16] Lu J T, Zhu Y H. Research on Vague Evaluation Based on Loader Cab Man-Machine Inferface. Applied Mechanics and Materials, 2011; 145: 510–514.

[17] Xie R H, Wu X P, Hu D H, Luo D H. An analysis of the vibration response of concrete gravity dams based on the state theory. China Rural Water Conservancy and Hydropower, 2016(11): 56–159.

[18] Qiu J, Wang D L, Ma Y L. Unified digital model of gear train analysis based on state space. Journal of Dalian University of Technology, 2021; 61(1): 52–59.

[19] Yasrebi M, Rafe V, Parvin H, Nejatian S. An efficient approach to state space management in model checking of complex software systems using machine learning techniques. Journal of Intelligent & Fuzzy Systems, 2019; 38(2): 1761–1773.

[20] Zhao X X. Research on dynamic traffic volume prediction based on state space model. Value Engineering, 2023; 42(34): 142–144.

[21] Li S, Su L B, Song S X. Review of studies on psychological workload of workers in man-machine system. Journal of Beijing Jiaotong University (Social Science edition), 2010; 9(3): 54–58.

[22] Pan C T, Hu J P. Research on the improvement of the barrel leakage algorithm under cloud computing. Silicon Valley, 2014; 7(16): 38–39,36.

[23] Bian L. An ergonomic study of the mental load. Vitality, 2010; 20: 127–128.

[24] Shi R, Liang Y W, Peng X. Mental load effect on the driver's stimulus detection. Journal of Human Ergonomics, 2023; 29(4): 76–81.

[25] Li J B, Xu B H, Tian X H. Construction of a prediction model of cognitive load in human-machine interaction process. Acta Psychologica Sinica, 2010; 42(5): 559–568.

[26] Zhong W J, Xu H M, Xu A. Comfort analysis and evaluation of man-machine system in tractor cab based on CATIA. Journal of Jiangsu University (Natural Science Edition), 2017; 38(1): 47–51.

[27] Hu D S, Zhu Z L. The reliability and validity test of the questionnaire based on SPSS and AMOS —A case study on the relationship among mathematical anxiety, mathematical attitude and mathematical self-efficien. Educational Measurement and Evaluation, 2020; 238(11): 3–7, 28.

[28] Chen W. Controllability and observability of flow-conservation transportation networks with fractional-order dynamics. MA dissertation. Chongqing: Chongqing Jiaotong University, 2022; 5. 65 p. doi: 10.27671/d.cnki.gcjtc.2022.001094 (in Chinese)

[29] Hou Y Q, Wu D. Small signal modeling and stability analysis for DC / DC. Journal of Huaihai Institute of Technology (Natural Science Edition), 2018; 27(1): 21–25.